A cloud-point extraction-chromogenic system for copper(II) based on 1-(2-thiazolylazo)-2-naphthol

T. S. Stefanova-Bahchevanska[1], R. S. Ahmedov[1], S. Zaruba[2], V. Andruch[3],
V. B. Delchev[1], L. K. Dospatliev[4], K. B. Gavazov[1,5*]

[1]*University of Plovdiv Paisii Hilendarski, Plovdiv, Bulgaria;*
[2]*Oles Honchar Dnipropetrovsk National University, Dnipro, Ukraine;*
[3]*Pavol Jozef Šafárik University in Košice, Košice, Slovak Republic;*
[4]*Trakia University, Stara Zagora, Bulgaria;* [5]*Medical University of Plovdiv, Plovdiv, Bulgaria*

A cloud point extraction-chromogenic system, containing Cu^{II}, 1-(2-thiazolylazo)-2-naphthol (TAN), and Triton X-100 (TX) was investigated. The optimum conditions for Cu^{II} extraction and spectrophotometric determination were found: absorption maximum (565 nm), concentration of TAN (4×10^{-5} M), mass fraction of TX (2.5%), pH (6.0), and incubation time (65 min). The molar absorptivity, limit of detection, linear working range, and fraction extracted were 2.9×10^5 dm^3 mol^{-1} cm^{-1}, 2.2 ng cm^{-3}, 7.2 – 380 ng cm^{-3} and 91%, respectively. The composition of the extracted complex is 1:2 (Cu:TAN). Its structure was optimized at the BLYP/aug-cc-pVDZ level of theory. The electron spectrum of the compound was simulated using Lorentzian band shape and compared with the experimental one.

Keywords: Cloud Point Extraction, Copper(II), Azo Dye, Spectrophotometry, TDDFT calculations, CPE

INTRODUCTION

Copper is a first row transition element from Group 11 with average content in the Earth's crust of 50 ppm [1]. It is a soft, malleable, and ductile metal with high electrical and thermal conductivity. Two early periods of the human history – Copper Age and Bronze Age – are closely related to this element. Nowadays, copper is considered as one of the most widely produced metals [2]. It is broadly used in electrical equipment and appliances, electrical transmission and communication wires, roofing and plumbing, industrial machinery, coins, pigments, micronutrients, etc. [1, 2].

Copper is an essential trace element to living organisms that performs a number of fundamental physiological functions. In humans, copper is the third most abundant trace element (after iron and zinc). Copper deficiency can cause anaemia, neutropenia, osteoporosis, hypopigmentation, increased incidence of infections, hyperthyroidism, and abnormalities in glucose and cholesterol metabolism. Because of difficulties in establishing the recommended dietary intake of copper, the National Research Council [3] has published a safe range in adults of 1.5–3 mg day^{-1}. At higher levels copper can be toxic [4].

Various methods have been used for copper determination. Sample preparation approaches which can improve significantly the characteristics of the determination are the extraction and microextraction techniques, such as liquid-liquid extraction (LLE) [5-7], solid phase extraction (SPE) [8-10], suspended droplet solvent microextraction (SDSME) [11], homogeneous liquid-liquid microextraction (HLLME) [12], dispersive liquid-liquid microextraction (DLLME) [13,14], and cloud point extraction (CPE) [15-23].

CPE is a modern alternative of LLE [24] which is consistent with the principles of "Green Analytical Chemistry" [25, 26]. It was introduced for the first time by Watanabe and Tanaka in 1978 [27] and a lot of scientists are oriented today towards its application for copper analysis [24]. A prerequisite for successful implementation of CPE is relatively high hydrophobicity of the analyte. That is why it is necessary to convert it into hydrophobic form, e.g. by complexation with chelating organic ligands. When using azo dyes as chelating reagents [24, 28], it is possible CPE to be combined with spectrophotometry – a simple and sensitive analytical method, which does not require expensive equipment and is therefore preferred in many laboratories [6].

The aim of this work was to investigate the CPE-chromogenic system for copper(II) containing 1-(2-thiazolylazo)-2-naphthol (TAN), acetate buffer, and Triton X-100 – a non-ionic surfactant with higher and more convenient in some aspects cloud-point temperature than the most utilized Triton X-114 [24, 29]. In addition, we used TD DFT calculations to optimise the structure of the extracted complex, to find its vertical excitation energies and simulate an electron spectrum for

direct comparison with the experimental one. Such calculations can be of help to better understand the system behaviour. Moreover, they have the potential to allow researchers to reduce the number of experiments on the selection of dyes and to predict in which direction the synthesis of new analytical reagents should be moved.

EXPERIMENTAL

Reagents and chemicals

A stock solution containing 2×10^{-2} M of Cu^{II} was prepared by dissolving $CuSO_4 \cdot 5H_2O$ (Sigma-Aldrich, Schnelldorf, Germany, purum p.a.) in water and standardizing by EDTA titration [7]. The working Cu^{II} solution (2×10^{-4} M) was prepared by suitably diluting with water. The ligand TAN (Fluka AG, Buchs, Switzerland, puriss. p.a.) was dissolved in ethanol, $c_{TAN} = 2 \times 10^{-3}$ M. Acetate buffer solutions were prepared by mixing 0.1 M aqueous solutions of CH_3COONa and CH_3COOH at appropriate ratios. Triton X-100 (electrophoresis grade) was purchased from Fisher Scientific, USA; 14% intermediate aqueous solutions of this reagent were prepared. Doubly distilled water was used through the work.

Instrumentation

A Camspec M508 spectrophotometer (United Kingdom), equipped with 0.5 and 1.0 cm path-length cells, was used for the spectrophotometric measurements. CPE was carried out in a home-made thermostated water bath heated on a ceramic heater Diplomat DPL CS-H20A9 (Bulgaria). The weighing was made with an electronic analytical balance (Kern, ABJ, Germany). A HANNA HI-83141 pH meter (Romania) was used for pH measurements.

Procedure for establishing the optimum CPE-spectrophotometric conditions

Various amounts of Triton X-100 solution (14%; 2 – 14 g), Cu^{II} working solution (0.1 – 2.5 cm³), buffer solution (3.0 cm³; pH ranging from 3.8 to 6.7), and TAN solution (0.05 – 1.8 cm³) were placed into 50 cm³ centrifuge test tubes. The solution volume was made to 50 cm³ with water. Then the test tubes were heated above the cloud point temperature (*ca.* 65°C) in 85°C water bath for 15-105 min. After the heating, the samples were

cooled in a freezer for 45 min (at −20°C) and the upper aqueous layers were decanted by inverting the tubes [30, 31]. Water was added to the viscous surfactant-rich phases to a total mass of 5 g and the mixtures were carefully heated for homogenization. Aliquot of the obtained solutions was transferred into the spectrophotometer cell and the absorbance was read against corresponding blank test.

Calculations

The ground-state equilibrium geometry of the copper complex was optimized at the BLYP level of theory and cc-pVDZ basis functions with no symmetry and geometry restrictions. Subsequently at the same level the vertical excitation energies of the compound were calculated. GAUSSIAN 03 program package [32] was used. Visualization of the optimized structure was done with the ChemCraft software [33].

RESULTS AND DISCUSSION

CPE-spectrophotometric optimisation

Wada and Nakagawa [34] investigated some o-(2-thiazolylazo)-phenol derivatives as metal indicators for copper. They found that TAN forms CuL^+ chelate with an absorption maximum at 578 nm and a stability constant of $10^{11.9}$. However, our CPE experiments showed that the absorption maximum position depends on the TAN concentration in the aqueous phase. At low TAN concentrations, the maximum is close to that previously reported [34] (Fig. 1, curve 2). On the other hand, at $c_{TAN} > c_{Cu(II)}$ there is a tendency the maximum to be shifted hypsochromically (by 10-20 nm) and split by a narrow minimum (at *ca.* 562 nm; Fig. 1, curve 1) which could be attributed to a change in the complex composition. This gave us an idea to examine this phenomenon in more detail.

Our further optimisation experiments included the following steps: (i) choice of the TAN concentration; (ii) choice of pH of the aqueous phase; (iii) choice of the Triton X-100 mass fraction; and (iv) choice of the incubation time. To achieve reliable optimisation, these steps were repeated. The final step optimisation results are shown in Figs. 1 – 3 and the recommended optimum conditions are summarized in the Table 1.

Table 1. CPE-spectrophotometric optimization of the Cu^{II} – TAN – Triton X-100 system

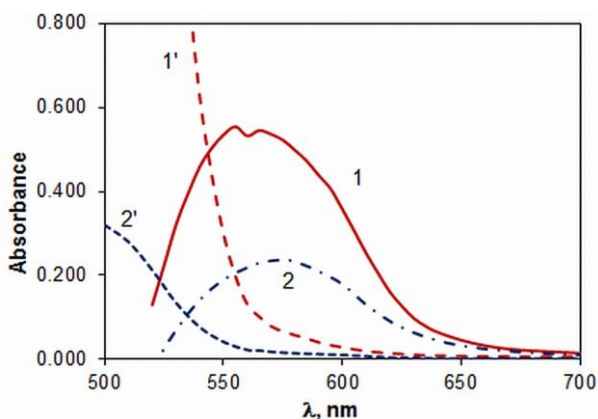| Parameter	Optimization range	Optimal value	Figure
Wavelength, nm	Visible region	565	Fig. 1
Concentration of TAN, M	$(0.2 – 7.2) \times 10^{-5}$	4.0×10^{-5}	Fig. 2
pH of the aqueous phase	3.8 – 6.7	6.0	Fig. 3
Incubation time, min.	15 – 105	65	–

Fig. 1. Absorption spectra: (1 and 2) Cu-TAN against blank; and (1' and 2') corresponding blanks against water. Conditions: $c_{Cu(II)} = 4 \times 10^{-6}$ M, pH = 6.0, $w_{triton} = 2.5\%$, l = 0.5 cm. $c_{TAN} = 4.0 \times 10^{-5}$ M (1 and 1') or 4.0×10^{-6} M (2 and 2').
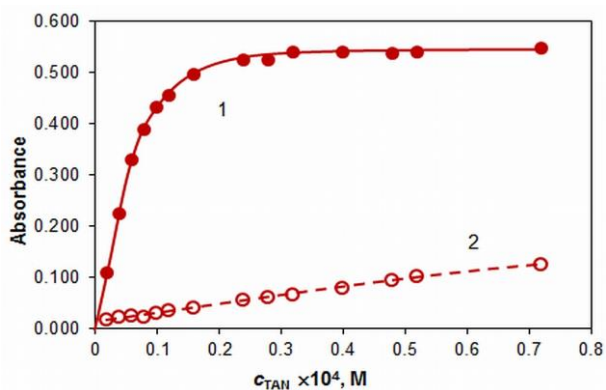

Fig. 2. Absorbance of the extracted complex (1) and blank (2) vs concentration of TAN. $c_{Cu(II)} = 4 \times 10^{-6}$ M, pH = 6.0, $w_{triton} = 2.5\%$, $\lambda = 565$ nm, l = 0.5 cm.
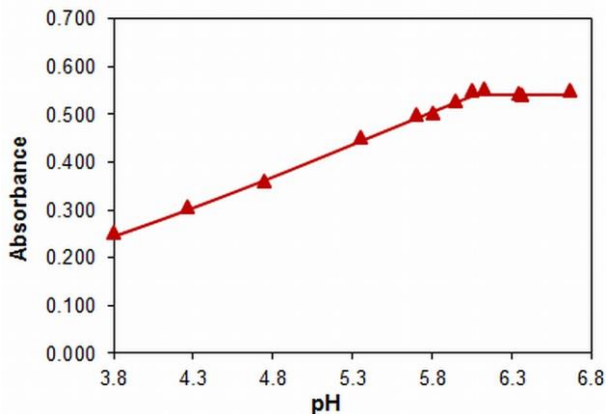

Fig. 3. Absorbance of the extracted complex vs pH. $c_{Cu(II)} = 4 \times 10^{-6}$ M, $c_{TAN} = 4 \times 10^{-5}$ M, $w_{triton} = 2.5\%$, $\lambda = 565$ nm, l = 0.5 cm.

Complex composition

The molar TAN:Cu^{II} ratio was determined by several methods [35] based on the saturation curve presented in Fig. 2, namely the equilibrium shift method (Fig. 4, line 2), Bent-French method (Fig. 4, line 1), straight-line method of Asmus (Fig. 5), and molar ratio method (Fig. 6). Based on the

40

obtained results, we can make the following conclusions: i) 2:1 (TAN:Cu^{II}) complex is extracted when $c_{TAN} > c_{Cu(II)}$; and ii) 1:1 complex is co-extracted when TAN concentration is very low ($c_{TAN} < c_{Cu(II)}$).
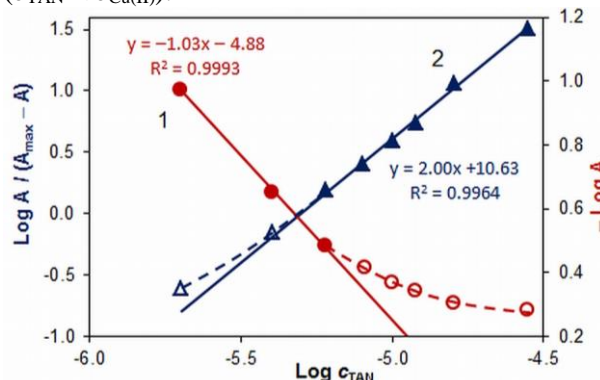

Fig. 4. Determination of TAN-to-Cu^{II} molar ratio by the Bent-French method (straight line 1; right ordinate) and the equilibrium shift method (straight line 2; left ordinate).
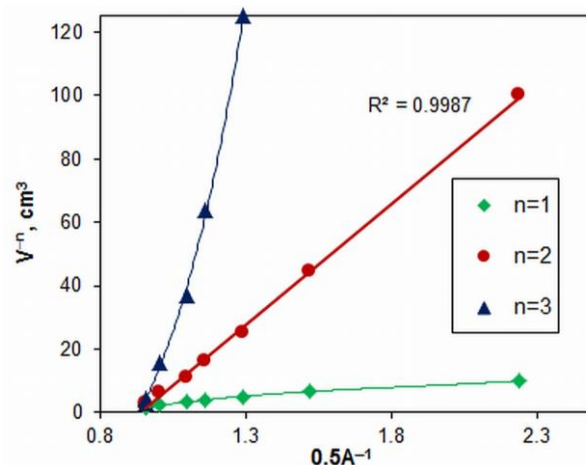

Fig. 5. Determination of TAN-to-Cu^{II} molar ratio by the straight-line method of Asmus.
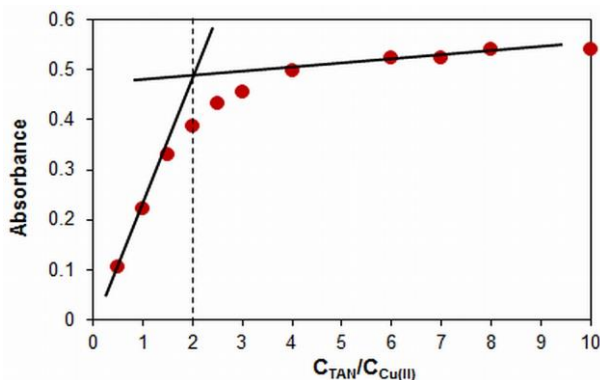

Fig. 6. Determination of TAN-to-Cu^{II} molar ratio by the molar ratio method.

Consequently there is a difference in the complex composition in aqueous medium (1:1, reported by Wada and Nakagawa [34]) and in surfactant-rich phase (2:1, at the optimum

conditions reported in this work). Similar differences have been reported by our group for the liquid-liquid extraction of coordination compounds containing azo dyes [31]. However, there are still not enough comparisons from this type (aqueous phase – surfactant-rich phase) for CPE. Generally speaking, authors aimed at developing analytical methodologies often neglect the possible change in the complex composition after CPE.

Extraction equation and equilibrium constant

The following equation could be proposed for the CPE process under the optimum conditions.

$$Cu^{II}_{(aq)} + 2HTAN_{(aq)} \Leftrightarrow [Cu^{II}(TAN^-)_2]_{(srp)} + 2H^+_{(aq)}$$
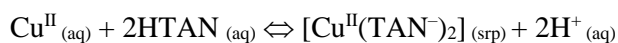
In this equation aq means aqueous phase, srp means surfactant rich phase, and HTAN is the protonated form of TAN (which dominates at pH_{opt} [24]). The equilibrium constant characterizing this equation was calculated by two methods: Holme-Langmyhr method [36] (Log K = 11.6 ± 0.4; N = 9) and Harvey-Manning method [37] (Log K = 11.7 ± 0.2; N = 3). As can be seen, the results are statistically indistinguishable.

Analytical characteristics

A calibration graph was constructed to estimate the applicability of the investigated CPE-chromogenic system for determination of Cu^{II}. Table 2 summarizes the obtained analytical characteristics. The fraction extracted (*E*) was calculated by comparing the absorbance values at the optimum conditions for single and triple extractions. The relatively high value for this type of extraction (*E*% = 91 ± 1; N = 3) could be attributed to (i) high stability of the resulting complex; and (ii) high hydrophobicity due to the incorporation of two moles of the reagent in the coordination entity.

Table 2. Statistical analysis of the calibration graph

Parameter	Value
Apparent molar absorptivity (ε), dm^3 mol^{-1} cm^{-1}	2.9×10^5
Linear calibration range, ng cm^{-3}	up to 380
Slope ± Standard deviation, $A \, \mu g^{-1}$ cm^3	2.13±0.02
Intercept ± Standard deviation, A	0.010±0.005
Correlation coefficient	0.9995 [a]
Limit of detection (LOD), ng cm^{-3}	2.2 [b]
Limit of quantification (LOQ), ng cm^{-3}	7.2 [b]

[a] nine standards used

[b] Defined as $3\sigma_{blank}$/b (LOD) or $10\sigma_{blank}$/b (LOQ), where b is the slope of the calibration plot

Optimized ground-state equilibrium geometry

The optimized structure of the copper complex is shown in Fig. 7. It shows two almost perpendicular one to other planar TAN$^-$ anions: <C4N1CuN6 = C17N4CuN3 = 90.6º. They are bonded with the oxygen and nitrogen (N1, N3, N4, and N6) atoms to the central Cu^{II} ion. The bonding leads to the formation of a coordination compound with a structure of non-regular octahedron. Due to the structural characteristics of the ligand and the strong repulsion of the lone electron pairs of the oxygen and nitrogen atoms, two of the coordination bonds are longer than the remaining: N6-Cu = 2.321 Å and N3-Cu = 2.313 Å. The angles N1CuN4, O2CuN6, and O1CuN3 are as follows: 177.2°, 153.8°, and 153.9°.
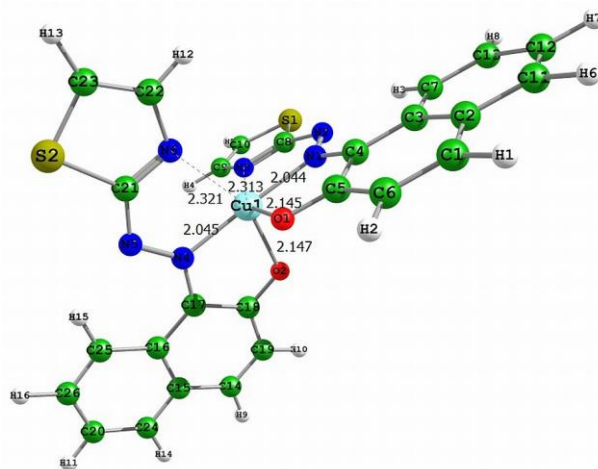

Fig. 7. Optimized structure of the copper complex at the BLYP/cc-pVDZ level of theory.

Theoretical spectrum

A theoretical spectrum of the complex in the visible range was modeled by the calculated electron transition lines and a Lorentzian broadening of the bands. When comparing it with the experimental spectrum one must take into account the following points: (i) the comparison makes sense only in the spectral range over *ca.* 520 nm as TAN (which is taken in excess under the experimental conditions) absorbs significantly at lower wavelengths; (ii) this effect cannot be compensated by reducing the concentration of ligand in the solution because the complex composition will be different (1:1); (iii) the experimental spectrum is registered in the solution (srf), while the theoretical one refers to the gas phase.

In Fig. 8 are compared the experimental spectrum (dotted line) and the theoretical spectrum (full line) of the compound normalized by unity. No scaling factor is required and it can be assumed that the overlap is satisfactory. The calculated main

absorption maximum involves the MOs shown in Fig. 9.

The molecular orbitals involved in the second most intensive peak at 486 nm are 139β and the one illustrated in Fig. 10. As seen, this molecular orbital is of π* type. In other words the electron transition 139β → 147β is a typical ligand field transition. The electron density shifts from the central metal ion towards the ligands.

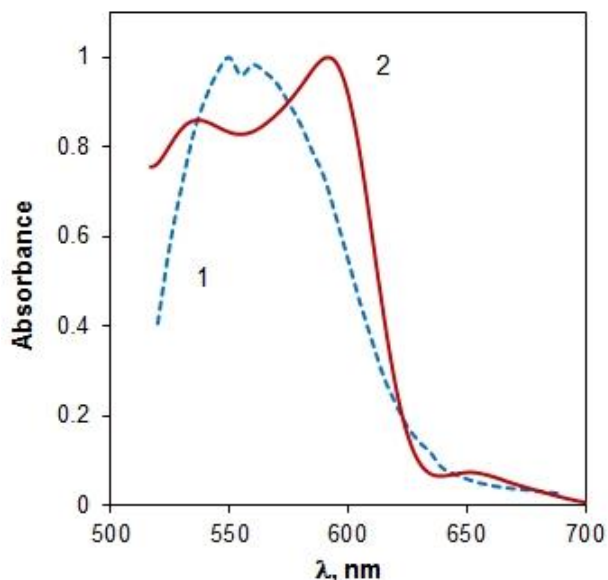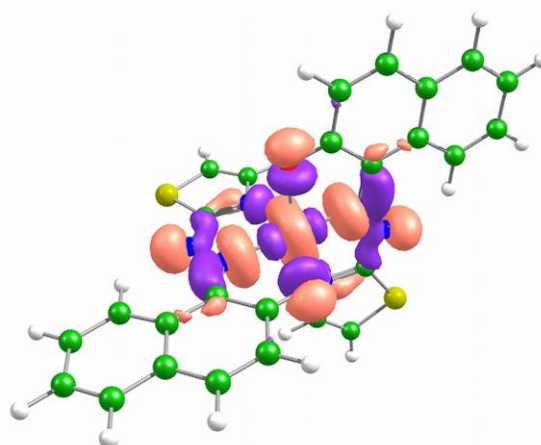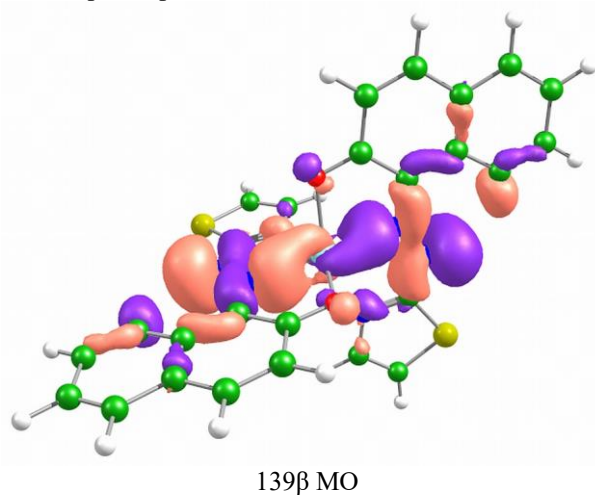**Fig. 8.** Experimental (curve 1) and theoretical (curve 2) absorption spectra.

139β MO

146β MO

Fig. 9. MOs involved in the electron transition responsible for the theoretically main absorption peak (oscillator strength f=0.1388).

147β MO
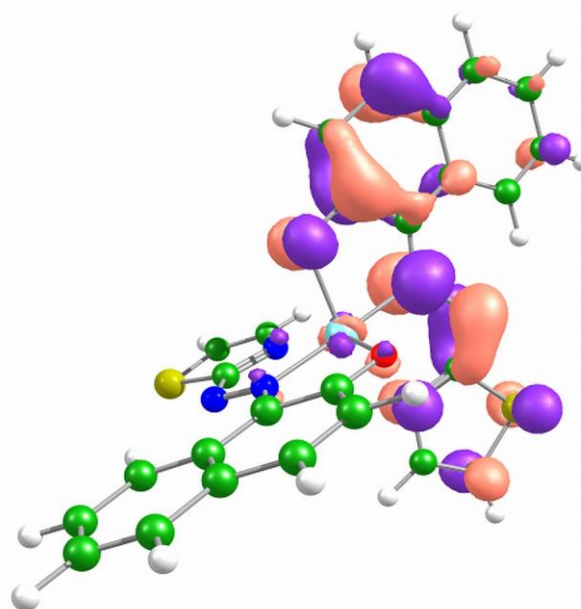
Fig. 10. MO involved in the electron transition 139β → 147β (oscillator strength f = 0.1202).

CONCLUSION

The cloud point extraction-chromogenic system Cu^{II} –TAN – TX was investigated in details and the optimum experimental conditions and analytical characteristics were found. The composition of the extracted complex was determined to be Cu:TAN = 1:2. Its structure was optimized and analyzed using the TD DFT method. An electron spectrum of the complex was simulated. The satisfactory fit between this spectrum and the experimental one is an indication for the correctness of the proposed structure.

REFERENCES

1. J. Emsley, Nature's building blocks: an AZ guide to the elements, Oxford University Press, New York, 2011.
2. A. Potysz, E. D. van Hullebusch, J. Kierczak, M. Grybos, P. N. L. Lens, G. Guibaud, *Crit. Rev. Environ. Sci. Technol.* **45**, 2424 (2015).
3. https://www.nap.edu/read/1349/chapter/11#227.
4. M. Araya, M. C. McGoldrick, L. M. Klevay, J. Strain, P. Robson, F. Nielsen, M. Olivares, F. Pizarro, L. Johnson, K. A. Poirier, *Reg. Toxicol. Pharmacol.* **34**, 137 (2001).
5. M. Thakur, M. K. Deb, *Talanta*, **49**, 561 (1999).
6. Z. Marczenko, M. Balcerzak, Metod'y spektrofotometrii v UF i vidimoj oblastyakh v neorganicheskom analize, Binom. Laboratoriya znanij, Moscow, 2007.
7. I. S. Balogh, M. Ruschak, V. Andruch, Y. Bazeľ, *Talanta*, **76**, 111 (2008).
8. A. Tobiasz, S. Walas, *Trends Anal. Chem.*, **62**, 106 (2014).
9. Ş. Tokalioğlu, V. Yilmaz, Ş. Kartal, *Environ. Monit. Assess.* **152**, 369 (2009).
10. A. Samadi, M. Amjadi, *Microchim. Acta*, **182**, 257 (2015).
11. N. Goudarzi, M. A. Chamjangali, E. Vatankhahan, A. Amin, *J. Anal. Chem.*, **69**, 1061 (2014).
12. N. Khorshidi, A. Niazi, *Separ. Sci. Technol.*, **51**, 1675 (2016).
13. A. Niazi, S. Habibi, M. Ramezani, *Arab. J. Chem.*, **8**, 706 (2015).
14. Z. Li, G. Yu, J. Song, Q. Wang, M. Liu, Y. Yang, *Water Sci. Technol.*, **67**, 247 (2013).
15. H. S. Ferreira, A. C. Santos, L. A. Portugal, A. C. Costa, M. Miró, S. L. Ferreira, *Talanta*, **77**, 73 (2008).
16. A. Pérez-Gramatges, A. Chatt, *J. Radioanal. Nucl. Chem.*, **294**, 163 (2012).
17. A.-N. Tang, D.-Q. Jiang, X.-P. Yan, *Anal. Chim. Acta*, **507**, 199 (2004).
18. E. L. Silva, P. dos Santos Roldan, M. F. Giné, *J. Hazard. Mater.*, **171**, 1133 (2009).
19. V. A. Lemos, M. S. Santos, G. T. David, M. V. Maciel, M. de Almeida Bezerra, J. Hazard. Mater., **159**, 245 (2008).
20. V. A. Lemos, M. S. Santos, M. J. S. dos Santos, D. R. Vieira, C. G. Novaes, *Microchim. Acta*, **157**, 215 (2007).
21. J. Chen, T. Khay Chuan, *Anal. Chim. Acta*, **450**, 215 (2001).
22. S. G. Silva, P. V. Oliveira, F. R. Rocha, *J. Brazil. Chem. Soc.* **21**, 234 (2010).
23. E. K. Yetimoğlu, O. A. Urucu, Z. Y. Gündüz, H. Filik, *Anal. Lett.*, **43**, 1846 (2010).
24. K. Pytlakowska, V. Kozik, M. Dabioch, *Talanta*, **110**, 202 (2013).
25. L. H. Keith, L. U. Gron, J. L. Young, *Chem. Rev.*, **107**, 2695 (2007).
26. P. T. Anastas, *Crit. Rev. Anal. Chem.* **29**, 167 (1999).
27. H. Watanabe, H. Tanaka, *Talanta*, **25**, 585 (1978).
28. V. A. Lemos, E. S. Santos, M. S. Santos, R. T. Yamaki, *Microchim. Acta*, **158**, 189 (2007).
29. W. L. Hinze, E. Pramauro, *Crit. Rev. Anal. Chem.*, **24**, 133 (1993).
30. K. Simitchiev, V. Stefanova, V. Kmetov, G. Andreev, N. Kovachev, A. Canals. *J. Anal. At. Spectrom.*, **23**, 717 (2008).
31. T. S. Stefanova, K. K. Simitchiev, K. B. Gavazov, *Chem. Pap.*, **69**, 495 (2015).
32. M. J. Frisch, et al., Gaussian 03; Gaussian, Inc.: Wallingford CT, 2004.
33. G. A. Zhurko, D. A. Zhurko, Chemcraft, ver.1.7 (build 382).
34. H. Wada, G. Nakagawa, *Bunseki Kagaku*, **14**, 28 (1965).
35. M. I. Bulatov, I. P. Kalinkin, Prakticheskoe rukovodstvo po fotokolorimetricheskim i spektrofotometricheskim metodam analiza, Khimiya, Leningrad, 1986.
36. A. Holme, F. J. Langmyhr, *Anal. Chim. Acta*, **36**, 383 (1966).
37. A. E. Harvey, D. L. Manning, *J. Am. Chem. Soc.*, **72**, 4488 (1950).